ORIGINAL ARTICLE

How to look for intracranial calcification in children with neurological disorders: CT, MRI, or both of them?

Davide Tonduti[1] · Anna Pichiecchio[2,3] · Carla Uggetti[4] · Stefania Maria Bova[1] · Simona Orcesi[3,5] · Cecilia Parazzini[6] · Luisa Chiapparini[7]

Abstract

Background Intracranial calcification (ICC) is an important diagnostic clue in pediatric neurology. Considering the radiation-induced cancer risk associated with computed tomography (CT), we aim to define the diagnostic value of magnetic resonance imaging (MRI) sequences sensitive to paramagnetic/diamagnetic substances in the detection of ICC, comparing with CT scanning.

Materials and methods We selected MRI and CT scans performed in children affected by neurological conditions associated with ICC referred to the participating centers between 2005 and 2018. Inclusion criteria were age at neuroradiological investigation < 18 years, availability of good quality CT positive for calcification, and MRI scan that included GE or/and SWI sequences, performed no more than 6 months apart.

Results Eighty-one patients were included in the study. CT and MRI scans were reviewed by consensus. MRI failed to detect ICC in 14% of the cases. Susceptibility-weighted imaging (SWI) was the best MRI sequence to use in this setting, followed by gradient echo imaging. In 19% of the cases, CT could have been avoided because the identification or monitoring of ICC has not been necessary for the clinical management of the patient.

Conclusion In the diagnostic workup of pediatric-onset neurological disorders of unknown cause, the first step to look for ICC should be an MRI that includes SWI and GE sequences. If ICC is absent on MRI, brain CT scanning should be performed at least once. When the identification or monitoring of ICC is unlikely to add information useful for patient's follow-up or treatment, we recommend not performing CT scanning.

Keywords Brain MRI · Brain CT · Leukodystrophy · Leukoencephalopathy · Intracranial calcification · Aicardi-Goutières syndrome

---

Davide Tonduti and Anna Pichiecchio equally contributed to this work.

Cecilia Parazzini and Luisa Chiapparini equally contributed to this work.

✉ Davide Tonduti
davidetondu@hotmail.com

1 Child Neurology, Unit - COALA (Center for Diagnosis and Treatment of Leukodystrophies), V. Buzzi Children's Hospital, Via Castelvetro 32, 20154 Milan, Italy

2 Neuroradiology Unit, IRCCS Mondino Foundation, Pavia, Italy

3 Department of Brain and Behavioral Sciences, University of Pavia, Pavia, Italy

4 Neuroradiology Unit, Department of Radiology, ASST Santi Paolo E Carlo, Milan, Italy

5 Child and Adolescent Neurology Department, IRCCS Mondino Foundation, Pavia, Italy

6 Paediatric Radiology and Neuroradiology Department - COALA (Center for Diagnosis and Treatment of Leukodystrophies), V. Buzzi Children's Hospital, Milan, Italy

7 Neuroradiology Unit, Fondazione IRCCS Istituto Neurologico Carlo Besta, Milan, Italy

Introduction

In clinical practice, the identification of specific neuroradiological patterns and features is crucially important in the diagnostic workup of neurological disorders. Intracranial calcification (ICC) is a common finding in normal aging, whereas it is very rarely observed in healthy children [1, 2]. The presence of ICC in children should always be considered pathological until proven otherwise [1, 3] and sometimes represents a sign that narrows down the differential diagnoses [1]. Collectively, pediatric-onset neurological disorders with ICC constitute a heterogenous group of conditions that include acquired disorders, such as congenital infections or brain tumors, genetic static syndromes, such as Adams Oliver Syndrome, and progressive encephalopathies, such as Cockayne syndrome (CS), Krabbe disease (KD), and some rare genetic interferonopathies such as Aicardi-Goutières syndrome (AGS) [1, 2, 4]. Central nervous system calcification deposits usually contain calcium hydroxyapatite ($Ca10 [PO4]6 [OH]2$) as a major component; zinc, iron, and magnesium are other possible components [5]. The mechanism underlying calcium deposition in the brain and spine is still a matter of debate, although a dysfunction in small cerebral blood vessels, including pericytes, has been suggested to play a key role in many cases [6, 7].

It has previously been recommended that CT scans, so far considered the gold standard for ICC detection, should be performed in children affected by leukoencephalopathies of unknown origin [3]. For the detection of ICC, ultrasound imaging may be used in newborns for its high sensitivity, even if the specificity is low [8]. On conventional T1- and T2-weighted MR sequences, the detection of ICC may be a challenge. The use of T2*-weighted or gradient echo (GE) sequences has considerably increased the sensitivity of MRI to ICC [3, 9], and moreover, susceptibility-weighted imaging (SWI), a 3D GE technique with high spatial resolution, has been reported to be the most suitable MRI approach for identifying and quantifying ICC differentiating calcification from blood products [10–12]. Few studies have already compared the diagnostic efficacy of MRI versus CT scan, for ICC detection, also in small pediatric samples and potentially SWI phase images might allow the same level of ICC detection as CT images [9], given the radiation exposure of the latter.

With our study, we aim to define the diagnostic value of magnetic resonance imaging (MRI) sequences sensitive to paramagnetic/diamagnetic substances in the detection of ICC, comparing with CT scanning. Moreover, we tried to identify in which cases CT exam should be considered diagnostically crucial keeping in mind that, as compared to adults, children are known to be at a greater risk for developing radiation-associated cancer [13].

Materials and methods

In order to make a qualitative comparison between CT and MRI scans with GE and/or SWI sequences, the neuroradiological reports from the neuroradiological databases of the four Italian centers involved in the study (Vittore Buzzi Children's Hospital in Milan, Casimiro Mondino Neurological Institute in Pavia, Carlo Besta Neurological Institute in Milan, San Carlo Hospital in Milan) were screened in order to select a set of "CT/MRI couple" meeting the following criteria: (1) age at examination < 18 years, (2) studied between 2005 and 2018, (3) presence of cerebral calcification at CT scan, (4) availability of good-quality MRI scan with GE and/or SWI sequences, performed no more than 6 months apart,

Scans were performed on a 1.5 T MRI scanner (Philips Achieva Healthcare, Eindhoven, the Netherlands; Siemens Avanto, Erlangen, Germany), 3 T MRI scanner (Siemens Magnetom Skyra, Erlangen, Germany; Philips Achieva Healthcare, Eindhoven, the Netherlands) using spin echo (SE) T1 and turbo spin echo (TSE) T2-weighted images, fluid-attenuated inversion recovery (FLAIR), and GE and SWI sequences. Brain CT scans were performed without a contrast medium (Somatom CT scanner, Siemens, Erlangen, Germany; Brilliance CT, Philips, Eindhoven, the Netherlands; GE CT scanner, GE Healthcare system, Milwaukee).

ICC was defined as areas of hyperattenuation (> 100 HU) at CT [9], while on MRI they were recognized as hypointense areas on GE and, on SWI filtered phase images, as hyperintense (positive phase) for a right-handed system and hypointense (negative phase) for a left-handed system [14]. Lesions with varying signals on SWI were classified according to their dominant signal (70% in space).

All the images were reviewed by all the authors, who are clinicians or radiologists specialized in pediatric neurology and pediatric neuroimaging. Each exam was evaluated in the presence of the whole group. When the agreement was not immediately reached, the case was discussed and finally scored only when the whole group agreed on the response. A final agreement has been reached in all cases. MRIs and CTs were read at different time points with a randomized reading order and with a long enough washout phase in between, in order to avoid biases.

In the presence of different combinations of signal intensity on a single MRI scan (for instance some areas of ICC showing T1 hypersignal and T2 hyposignal, others presenting T1 and T2 hyposignal), the scan was scored two times, each time focusing on the areas showing the same signal combination. In the analysis of the data, each of these evaluations was considered a separate study. ICC on CT scans was classified by localization and type, in accordance with a previously proposed classification system [3]. The prevalent

signal for each ICC on T1- and T2-weighted images and on FLAIR, GE, and SWI sequences was established. For each MRI exam, we selected which was the sequence that better showed the presence of ICC mainly making a comparison between GE and SWI sequences. Lastly, in every single case, we also considered whether the CT scan provided any added diagnostic clinical value, that helped reach the diagnosis or changed the patient's clinical management. This evaluation was made after study scoring and was based on the combination of neuroradiological data and clinical information that were available for all included patients.

Results

General data

The neuroradiological records of 254 patients were consulted. Of these, 81 patients (42 males, 39 females) met the inclusion criteria.

Seven patients had MRI scans showing different combinations of signal intensity. As described in the methods, these scans were scored more than once. This resulted in a final total of 90 studies (88 brain and 2 spinal cord studies).

The MRI and CT studies were performed at a mean age of 6.7 ± 5.8 years (range: 1 month to 17.7 years); to underline, 9 subjects underwent MRI between the age of 1 and 12 months.

All the MRI studies included T1- and T2-weighted images. FLAIR sequences were available in all but two of the brain studies. All the 90 radiological studies included at least one SWI or GE sequence; GE sequences were performed in 76 studies and SWI in 32. Only SWI was done in 14 patients, only GE in 58 while 18 studies included both these types of sequence.

The clinical diagnoses in this population included the following: Aicardi-Goutières syndrome (AGS) (16 patients), brain tumor (17), unclassified neurodegenerative disease (12), congenital infection (5), unclassified congenital static encephalopathy (4), leukoencephalopathy with brainstem and spinal cord calcification (LBSC) (3), tuberous sclerosis (3), Sturge-Weber syndrome (3), Cerebral angiomatosis(2), small vessel stroke (2). The remaining diagnoses were all recorded in single cases (Table 1).

Table 1 Number of MRIs and patients and CT diagnostic value per diagnosis

Diagnosis	Number of MRIs	Number of patients	Added value of CT
Aicardi-Goutières syndrome	16	16	14 Yes **2 No**
Brain tumor	17	17	16 Yes **1 No**
Unclassified neurodegenrative disease	16	12	Yes
Congenital infection	**5**	**5**	**No**
Leukoencephalopathy with brainstem and spinal cord calcification (LBSC)	6	3	Yes
Unclassified static genetic encephalopathy	4	4	Yes
Tuberous sclerosis	**3**	**3**	**No**
Primary familial brain calcification	3	1	Yes
Sturge-Weber syndrome	**3**	**3**	**No**
Cocakyne syndrome	1	1	Yes
Hypoxic ischemic encephalopathy	**1**	**1**	**No**
Cerebral angiomatosis	2	2	Yes
KRIT1-related cerebral cavernous malformations (CCM1)	1	1	Yes
CYP2U1- related distoder	1	1	Yes
Pantothenate kinase-associated neurodegeneration (PKAN)	1	1	Yes
Hyperparatiroidism	1	1	Yes
Cortical dysplasia	1	1	Yes
Vascular malformation	1	1	Yes
Atypical Sturge-Weber syndrome	1	1	Yes
Small vessel stroke	**2**	**2**	**No**
Neonatal intraventricular hemorrhage	**1**	**1**	**No**
Meningoencephalitis	1	1	Yes
Neonatal hypoglycemia	**1**	**1**	**No**
Prenatal brain injury	1	1	Yes
Total	90	81	

CT features: ICC topography and morphology

Intracranial calcification was observed in the cerebral cortex in 16 cases, the subcortical white matter in 31, the deep white matter in 23, the periventricular white matter in 19, the corpus callosum in 4, the posterior limb of the internal capsule in 5, the anterior limb of the internal capsule in 1, the putamen in 23, the pallidal nuclei in 18, the caudate nuclei in 11, the thalami in 17, the midbrain in 3, the pons in 7, the medulla oblongata in 2, the cerebellar cortex in 4, the cerebellar white matter in 7, the dentate nuclei in 4, and the spinal cord in 2. In seventeen cases, ICC was localized into tumor tissue and therefore topographically classified as "intralesional." In one patient, it occurred in the site of a vascular malformation.

Spot calcification and blush-like calcification were each found in 51 studies, blush in 51, while rock calcification was found in 39. In 16, ICC was linear, in 12 gyriform, and band-like in 1.

MRI features of ICC

In the whole series, MRI failed to detect ICC in 13/90 studies (14%). These 13 cases were heterogeneous in terms of localization and etiological diagnosis, but concerned small ICC. CT had demonstrated the presence of small spot ICC in 8/13, gyriform in 3, linear and punctuate in 1, and blush in 1. Notably, no calcification was visible on three of the 18 MRI scans (17%) performed using both GE and SWI sequences, on 10 of the 58 (17%) performed with GE but not SWI, and on 1 of the 14 (7%) performed using SWI but not GE.

On T2-weighted images, ICC was visible on 43/90 scans (47%). The lesions appeared hypointense in 38/43 (88%), hyperintense on the scan of one patient affected by pantothenate kinase-associated neurodegeneration (PKAN), and presented a mixed hyper- and hypointense signal in four patients (1 with tuberous sclerosis, 1 with brain tumor, and 2 with unclassified neurodegenerative disease).

On FLAIR sequences, ICC was visible in 32/86 (37%) studies, and in these cases, the signal always matched that found on T2-weighted imaging.

On T1-weighted imaging, ICC was visible in 30/90 (33%) studies. The lesions appeared hyperintense in 18/30 (60%), hypointense in 10/30 (35%), and mixed (hyper- and hypointense) in two patients (1 with brain tumor and 1 with unclassified neurodegenerative disease). In 11 studies, ICC was visible on T1-weighted imaging (hyperintense in 7 and hypointense in 4) but not on T2-weighted imaging; conversely, in 24, they were visible on T2-weighted imaging (hypointense in 23 and mixed in 1) but not on T1-weighted imaging. Collectively, T1- and/or T2-weighted imaging demonstrated the presence of ICC in 54/90 studies (60%).

Intracranial calcification was visible on 62/76 (80%) of the GE and 28/32 (87%) of the SWI sequences, in both cases showing hypointense signal. As regards the 18 studies performed using both sequences, ICC was visible on both sequences in 14 and only on SWI in one. In 3/18 cases, no ICC was detected.

Figures 1 and 2 are examples of the neuroimages reviewed for ICC topography and morphology.

We considered as the best MRI sequence the sequence in which signal alteration was more easily referable to ICC.

When GE, but not SWI, was available (58 studies), we considered the following to be the best techniques: GE in 42/58 (72%), T2 in 5/58 (9%), and T1 in 2/58 (3%); in the other 9 (16%), ICC was not detected. When SWI but not GE was available (14 studies), the best technique was SWI in 12/14 (85%), while ICC was not detected in the remaining 2 (15%). In the group of 18 studies performed using both SWI and GE, SWI was deemed to be the best MRI technique in 10/18 (55%), GE in 4/18 (22%), and T2 in 1/18 (6%); in 3/18 (17%), no MRI sequence detected ICC.

Comparison between CT and MRI

It is interesting to note that in 4/90 studies MRI was deemed better in detecting calcification shape and dimension, and in 4/90, CT and MRI were considered equal. In the other 82/90, we confirmed our starting assumption based on literature that CT is the best technique for detecting ICC.

Regarding the clinical relevance of CT scanning, we considered that CT was useful and therefore diagnostically necessary in 71/90 (79%) patients for clinical management, while it could have been avoided in 19 (21%).

Discussion

In this study, we described the MRI features of ICC in a series of 81 pediatric patients affected by neurological conditions. Our results confirm that SWI is the best MR sequence in detecting ICC, mainly compared with the GE sequence. Nevertheless, MRI studies were not able to demonstrate the presence of calcification in 14% of cases. That was likely due to the small dimension of ICC in those cases and suggests that, even when SWI and GE are negative for ICC, CT is still necessary to exclude its presence.

Calcium is a diamagnetic substance and has a very low magnetic susceptibility compared with the surrounding tissue. Furthermore, ICC, depending on its structural and chemical characteristics, may appear as either high or low signal on both T1- and T2-weighted sequences and it can result in difficulty to differentiate it from hemosiderin, especially on GE sequences. In fact, on GE sequence, ICC is seen as areas of low signal dropout, but this signal abnormality
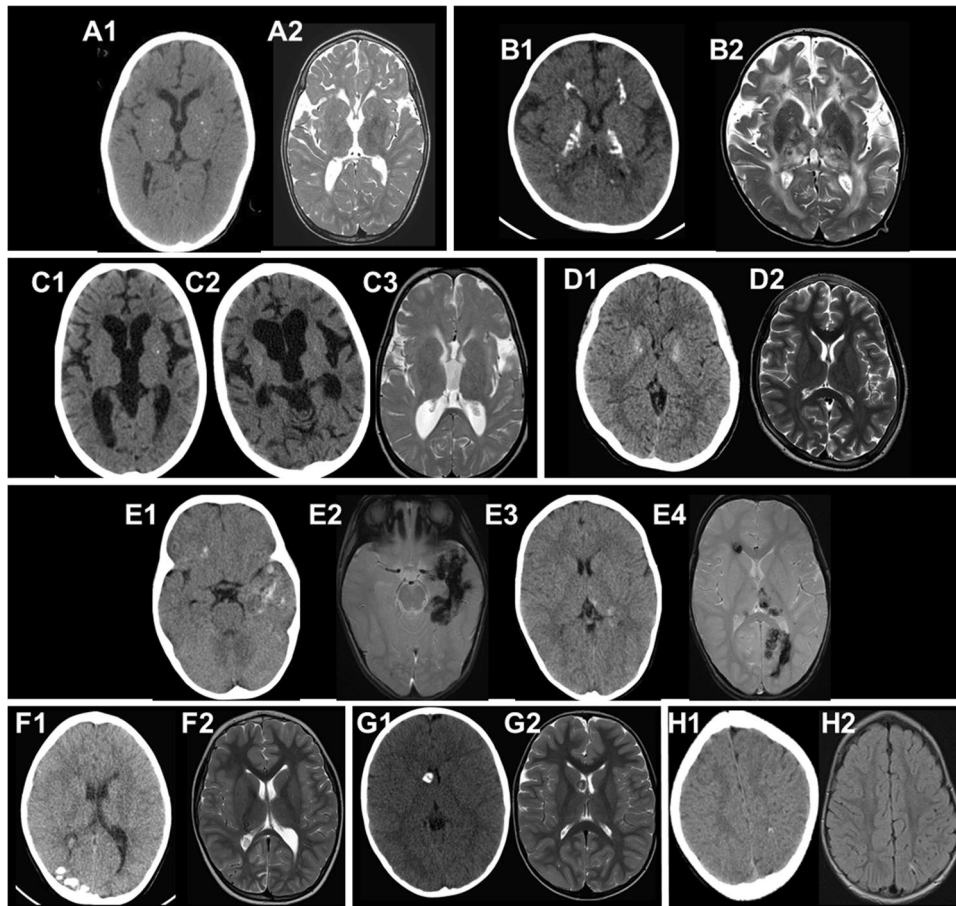
Fig. 1 Examplesof the neuroimages reviewed for ICC topography and morphology. A1–2.CT image(1) and axialMRT2-weighted image (2) of pt 14, affected by AGS, at 4.6 years. The imagesshow small punctate calcificationsin the basal ganglia and thalami bilaterally. These are less visible on theT2-weighted images. B1–2.CTimage (1) and axial MRT2-weighted image (2) of pt 23, affectedleukoencephalopathy with brainstem andspinal cord calcification, at 2.6 years of age. The images show diffusebilateral white matter hyperintensity, alsoinvolving the external and internal capsules and both thalami, with sparing ofthe U fibers, associated with bilateralrock calcification lesions in the anterior periventricular white matter, withslight predominance on the left side,and in the posterior limb of the internal capsules. C 1–3. CT image (1–2) andaxial MRT2-weighted image (3) of pt 35, affected by Cockayne syndrome, at age 8.5 years. The images showpunctate calcification of the putamen,which is a typical site in this disease, mainly on the left side and not clearlyvisible on the T2-weighted images.Note the slight hyperintensity of the deep white matter, which is related tohypomyelination, and the superficialand deep cerebral atrophy. D1–2. CT image (1) and MRT2-weighted image (2) of pt60, affected by hyperparathyroidism,at the age of 15.5 years. The CT image shows blush calcification of the pallidi-

and, partially,of the putamen can be seen on both sides. These features are not detectable onthe T2-weighted image.E1–4.Axial CT image (1–3) and MRT2-GE (2–4) of pt46, affected by KRIT1-relatedcerebral cavernous malformations(CCM1), at the age of 2.1 years. Linear andreticular calcification lesions arevisible in the areas ofthe cerebral cavernous malformations: frontal (1, 4), temporal (1, 2), thalamic(3, 4), and parietal (4); diffuse hypointensity isdetected on GE images, due to the "blooming artifact" and, probably, concomitantblood products.F1–2.CT image (1) and axial MRT2-weighted image(2) of pt 9, affected bySturge-Weber syndrome, at5.6 years of age. Rock and gyriform calcification lesions are evident on theposterior corticosubcortical region ofthe right hemisphere, associated with slight atrophy. Note a hypertrophic veinto the right thalamus on MRI. G1–2.CT image (1) and MRT2-weighted image (2) of pt 8, affected by tuberoussclerosis, at 5.1 years of age. A roundsubependymal focal calcification is evident at the level of the right Monro foramen,with an inhomogeneoussignal on MRI (2). H1–2. CT image (1) and axial MR FLAIR image (2) of pt 55, 20months of age,who suffered from neonatal hypoglycemia. A small gyriform corticalcalcification can be observed in the left parasagittalparietal cortex, associated with slight hyperintensity on T2 FLAIR image

can be due to either calcium or iron, while SWI sequences are able to differentiate between calcium and blood products, increasing the capability of MRI as a technique for evaluating ICC [11, 12]. To enhance the image contrast conferred

by the paramagnetic properties of blood products (such as deoxy-hemoglobin, intracellular methemoglobin, and hemosiderin), in comparison with the diamagnetic properties of calcium, SWI combines magnitude and phase data [15].
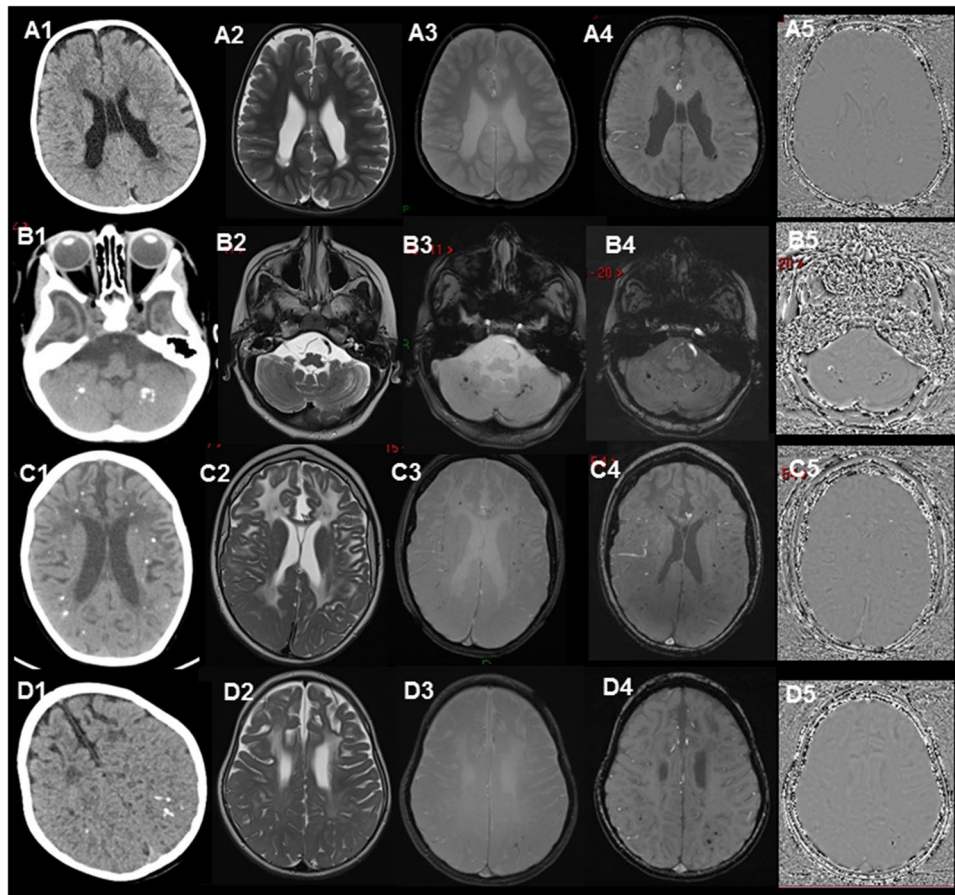
Fig. 2 ICC appearance on CT and on different MRI sequences. A1-5. CT image (1) and 3 T Siemens MR (left-handed) T2-TSE (2), T2-GE (3), SWI (4), and phase images (5) of Pt 30, affected by periventricular leukomalacia due to perinatal distress, at the age of 4 years. CT better depicts the posterior periventricular calcification lesions mixed with hemosiderin. On MRI sequences, even SWI, the calcification is not easily distinguishable from blood products. B1-5 and C1-5. CT image (1) and 3 T Siemens MR (left-handed) T2-TSE (2), T2-GE (3), SWI (4) and phase images of Pt 16, affected by AGS, at the age of 3 months, respectively at the level of the cerebellum (B) and corona radiata (C). Multiple punctate focal calcifications are evident in both cerebellar hemispheres on CT, well evident as hypointensity on T2-GE images. They are also clearly visible in the supratento-

rial regions on MR T2-weighted and T2*-weighted images, favored by contrast with the hyperintense white matter. On SWI (4–5) they have a predominant hypointense signal with "aliasing", or distortion artifact, on the phase image of the bigger cerebellar lesion on the right side and the frontal ones, which are not readily distinguishable from blood products. Nevertheless, clinical and MRI data together were sufficient to confirm the clinical suspicion, making CT unnecessary. D1-5 CT image (1) and 3 T Siemens MR (left-handed) T2-TSE (2), T2-GE (3), SWI (4), and phase images (5) of Pt 63, affected by AGS, at the age of 2.6 years. Punctate juxtacortical calcification in both parietal lobes on CT, not easily visible on T2, better distinguishable on GE, and even better on SWI as hypointense lesions (negative phase)

Specifically, calcification and blood products (nonheme iron) show opposite signal intensity; therefore, using veins as a reference on SWI filtered phase images, the signal from calcium is opposite to that coming from the paramagnetic veins [16]. The reading of SWI phase images is subject to possible pitfalls. Aliasing, which results in opposite intensities at the edges and the center of the lesion, is the main one. It can be reduced by shortening echo and/or double echo time, or by more appropriate phase conversion to local susceptibility [17]. The second pitfall is the appearance of both a negative and a positive phase surrounding a larger diamagnetic object; this problem can be overcome by reprocessing images in order to suppress local magnetic fields

or susceptibilities. A further limit to the application of this technique on a large scale is that correct interpretation of the images still relies on the expertise of the image reader.

Even if in our cases SWI showed a higher capability compared with GE in detecting ICC, however, an agreement was always reached about the evidence that lesions appeared more immediately visible and clearer on GE. For this reason, we suggest that both sequences should be included, when possible, in MRI protocols for ICC evaluation, although we are aware of the longer scan time.

We also observed that in the first year of life, when the white matter is not yet completely myelinated, ICC is readily seen as low signal spots also on T2wi, while they become

less visible with increasing age as myelination occurs. For this reason, in patients aged less than 12 months, MRI is often sufficient to disclose ICC avoiding CT scan mainly in this period of life in which exposure to ionizing radiation is more dangerous.

Furthermore, we noted that ICC in cerebellar hemispheres and spinal cord were better detectable on MRI than CT, probably because these are classical regions in which CT images are frequently degraded by bone artifacts of the posterior fossa and spinal canal.

The identification of calcification by CT scanning added relevant and necessary information in the patient diagnostic workflow in about three-quarters of the studies. It was instead deemed unnecessary in patients with congenital infection, Sturge-Weber syndrome, tuberous sclerosis, and also in AGS patients in whom clinical examinations and MRI studies have already provided enough information to address the diagnosis.

The study bears several limitations. Our sample is highly heterogenous including a large spectrum of genetic and acquired pathologies; a significant group is represented by AGS patients and this is explained by the fact that two of the participating centers are Italian referral centers for this disease (Casimiro Mondino Foundation in Pavia and Vittorio Buzzi Children's Hospital in Milan). The Mondino Foundation is also the scientific headquarters of the International Aicardi-Goutières Syndrome Association. Patients were retrospectively selected from four different Institutions; radiological examinations were performed following different protocols with different MR machine vendors; both GE and SWI MRI sequences were available in only some of the MR exams; all patients had ICC on CT scans; therefore readers were aware that ICC had to be found on MRI and was not blinded; intra- and interrater variability could not be obtained as the assessment of the images was in consensus by all the authors lacking blindness. Moreover, recent years have witnessed further development in the field of magnetic susceptibility imaging, namely regarding the quantification of signal changes through quantitative susceptibility mapping (QSM), being not dependent on local and orientation-dependent phase signals and probably superior to conventional SWI [9]. In our study, no patient performed QSM; however, also the interpretation of QSM images is subject to limitations, and more technical advances are needed in order to improve its diagnostic accuracy.

In conclusion, given the importance of looking for ICC, the first step in the diagnostic workup of pediatric-onset neurological disorders of unknown cause should be a careful evaluation of an MRI study that includes SWI sequences, as they demonstrated to have a higher capability compared with GE in detecting ICC. GE sequences should be performed only if SWI sequences are not at disposal or in case of lack of training. In patients with encephalopathy of undetermined etiology, but no ICC on MRI, brain CT scanning should be performed at least once, in agreement with previous studies [3]. In cases requiring radiological follow-up to monitor ICC evolution, MRI should be preferred to CT.

Declarations

Ethics approval and consents The study adheres to the principles of the Code of Ethics of the World Medical Association—Helsinki Declaration and concerns data gathered during routine diagnostic activity. The study was approved by the local ethics committee. The study complied with the institutional regulations for anonymized retrospective studies.

Conflict of interest The authors declare no competing interests.

References

1. Livingston JH, Stivaros S, Warren D, Crow YJ (2014) "Intracranial calcification in childhood: a review of aetiologies and recognizable phenotypes," (in eng). Dev Med Child Neurol 56(7):612–626. https://doi.org/10.1111/dmcn.12359

2. Tonduti D et al (2018) "Encephalopathies with intracranial calcification in children: clinical and genetic characterization," (in eng). Orphanet J Rare Dis 13(1):135. https://doi.org/10.1186/s13023-018-0854-y

3. Livingston JH, Stivaros S, van der Knaap MS, Crow YJ (2012) "Recognizable phenotypes associated with intracranial calcification," (in Eng). Dev Med Child Neurol. https://doi.org/10.1111/j.1469-8749.2012.04437.x

4. Donzuso G, Mostile G, Nicoletti A, Zappia M (2019) "Basal ganglia calcifications (Fahr's syndrome): related conditions and clinical features," (in eng). Neurol Sci 40(11):2251–2263. https://doi.org/10.1007/s10072-019-03998-x

5. Deng H, Zheng W, Jankovic J (2015) "Genetics and molecular biology of brain calcification," (in eng). Ageing Res Rev 22:20–38. https://doi.org/10.1016/j.arr.2015.04.004

6. McCartney E, Squier W (2014) "Patterns and pathways of calcification in the developing brain," (in eng). Dev Med Child Neurol 56(10):1009–1015. https://doi.org/10.1111/dmcn.12493

7. Zarb Y, Franzoso FD, Keller A (2019) "Pericytes in primary familial brain calcification," (in eng). Adv Exp Med Biol 1147:247–264. https://doi.org/10.1007/978-3-030-16908-4_11

8. Dykes FD, Ahmann PA, Lazzara A (1982) "Cranial ultrasound in the detection of intracranial calcifications," (in eng). J Pediatr 100(3):406–408. https://doi.org/10.1016/s0022-3476(82)80441-1

9. Chen W et al (2014) "Intracranial calcifications and hemorrhages: characterization with quantitative susceptibility mapping," (in eng). Radiology 270(2):496–505. https://doi.org/10.1148/radiol.13122640

10. Gupta RK et al (2001) "Differentiation of calcification from chronic hemorrhage with corrected gradient echo phase imaging," (in eng). J Comput Assist Tomogr 25(5):698–704

11. Yamada N, Imakita S, Sakuma T, Takamiya M (1996) "Intracranial calcification on gradient-echo phase image: depiction of diamagnetic susceptibility," (in eng). Radiology 198(1):171–178. https://doi.org/10.1148/radiology.198.1.8539373

12. Zhu WZ et al (2008) "Magnetic resonance susceptibility weighted imaging in detecting intracranial calcification and hemorrhage," (in eng). Chin Med J (Engl) 121(20):2021–2025

13. Chodick G, Kim KP, Shwarz M, Horev G, Shalev V, Ron E (2009) "Radiation risks from pediatric computed tomography scanning," (in eng). Pediatr Endocrinol Rev 7(2):29–36

14. Wu Z, Mittal S, Kish K, Yu Y, Hu J, Haacke EM (2009) "Identification of calcification with MRI using susceptibility-weighted imaging: a case study," (in eng). J Magn Reson Imaging 29(1):177–182. https://doi.org/10.1002/jmri.21617

15. Tong KA, Ashwal S, Obenaus A, Nickerson JP, Kido D, Haacke EM (2008) "Susceptibility-weighted MR imaging: a review of clinical applications in children," (in eng). AJNR Am J Neuroradiol 29(1):9–17. https://doi.org/10.3174/ajnr.A0786

16. Sahin N, Solak A, Genc B, Kulu U (2015) "Fahr disease: use of susceptibility-weighted imaging for diagnostic dilemma with magnetic resonance imaging," (in eng). Quant Imaging Med Surg 5(4):628–632. https://doi.org/10.3978/j.issn.2223-4292.2015.04.01

17. Ciraci S et al (2017) "Diagnosis of intracranial calcification and hemorrhage in pediatric patients: comparison of quantitative susceptibility mapping and phase images of susceptibility-weighted imaging," (in eng). Diagn Interv Imaging 98(10):707–714. https://doi.org/10.1016/j.diii.2017.05.004

Publisher's Note Springer Nature remains neutral with regard to jurisdictional claims in published maps and institutional affiliations.